

Acta Crystallographica Section D

Volume 70 (2014)

Supporting information for article:

The crystal structure of human interleukin-11 reveals receptor binding site features and structural differences from interleukin-6

Tracy L. Putoczki, Renwick C. J. Dobson and Michael D. W. Griffin

Table S1 Related to Figure 4. Comparison of IL-6 residues involved in binding GP130 with the corresponding residues of hIL-11. For consistency, only interface residues situated on helical elements have been compared, since loop segments may rearrange upon binding. For clarity, residue numbering for IL-6 is provided as in PDB ID 1ALU.

IL-6	IL-11	IL-11 alternative
	Site II	
Arg24	Ser41	Glu38
Lys27	Leu44	Ser41
Gln28	Leu45	Thr42
Arg30	Arg47	Leu44
Tyr31	Ser48	Leu45
Asp34	Ala51	Ser48
Glu110	Pro124	Thr128
Gln111	Glu125	Leu129
Arg113	Gly127	Ala131
Ala114	Thr128	Arg132
Met117	Ala131	Asp134
Ser118	Arg132	Arg135
Val121	Arg135	Arg138
Gln124	Arg138	Gln141
Phe125	Arg139	Leu142
Lys128	Leu142	Arg146
	Site III	
Asn45	Asp62	
Lys46	Lys63	
Gln156	Ala167	
Trp157	Trp168	
Leu158	Gly169	
Met161	Arg172	
Thr162	Ala173	
Leu165	Ala176	

^a Obtained by adjusting the position of IL-6 one helical turn toward the N-terminus of helix A of IL-11 relative to the calculated superposition shown in Figure 4A.

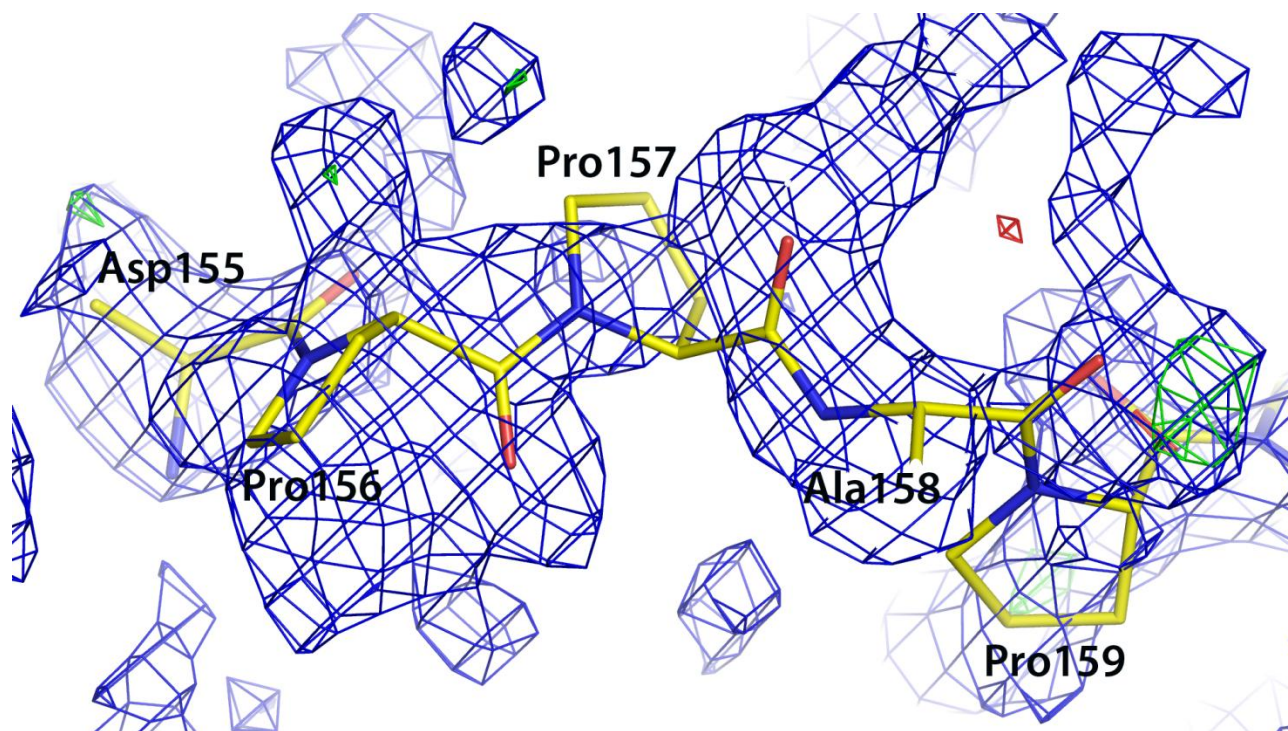


Figure S1 Related to Figure 1. Electron density for residues 155 to 159 of loop-CD. Density in this region of loop-CD was weak. However, continuous density at low sigma values provided sufficient information to allow tracing of the loop backbone and these residues were included in the model. $2F_o-F_c$ density is contoured at 0.5 sigma (blue mesh), F_o-F_c difference density is contoured at 3.0 sigma (green mesh) and -3.0 sigma (red mesh).

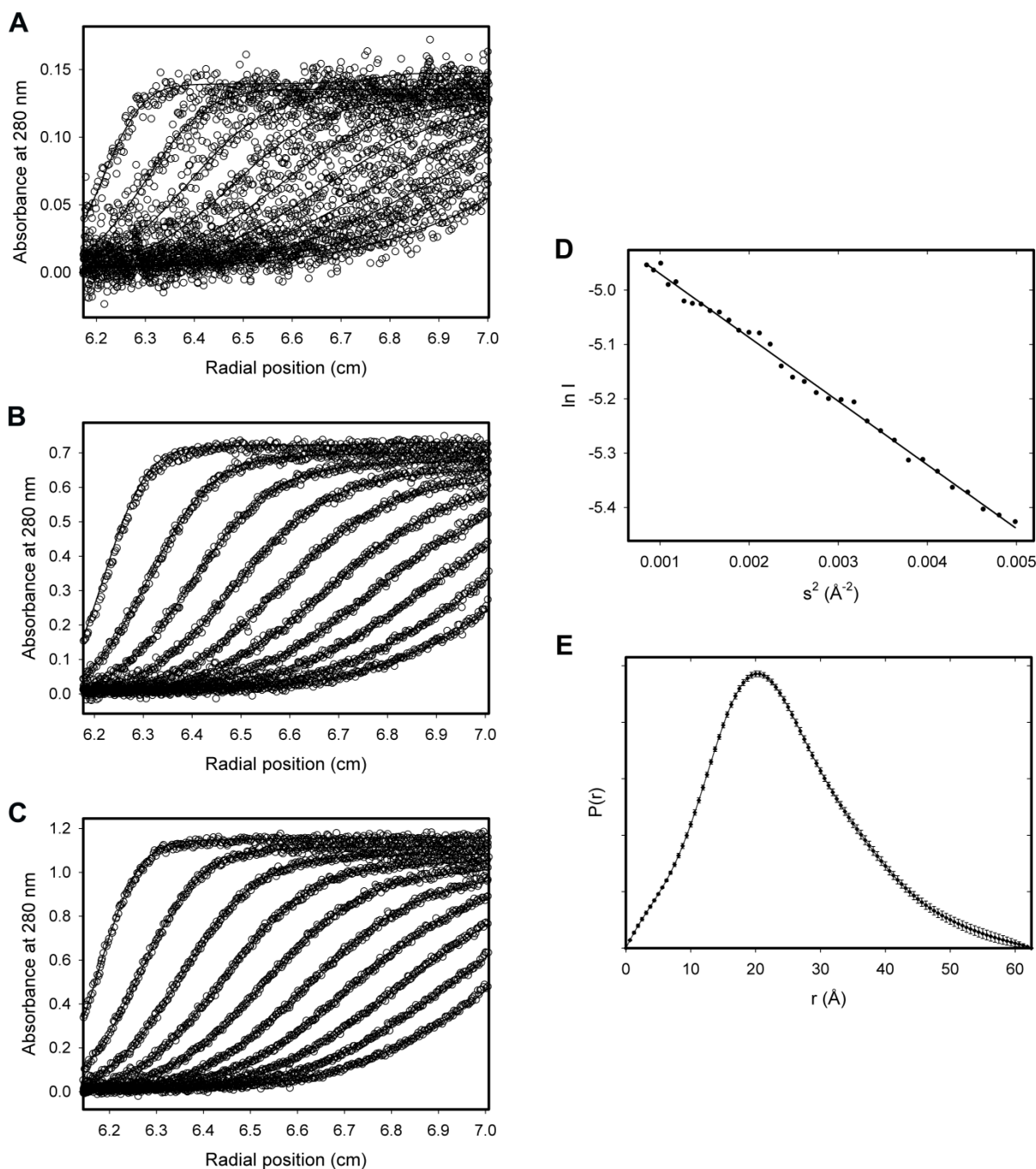


Figure S2 Related to Figure 2. A-C: Analytical ultracentrifugation sedimentation velocity data for hIL-11. Sedimentation velocity data were acquired at protein concentrations of 0.2 mg/ml (A), 0.6 mg/ml (B) and 1.0 mg/ml (C). Absorbance data were acquired at 280 nm and intervals of 10 min. Every fifth scan is shown for clarity. Raw sedimentation velocity absorbance data (open circles) are shown overlaid with best fits to a $c(s)$ continuous sedimentation coefficient distribution (solid lines). D: Guinier analysis of small angle X-ray scattering (SAXS) data for hIL-11. Raw scattering data shown in Figure 2B were plotted within s - R_g limits of 0.52 and 1.30. The linearity of the data indicates good sample homogeneity, with little or no aggregation of the protein. The fit to the data provides a radius of gyration (R_g) of $18.80 \pm 0.56 \text{ \AA}$ and I_0 of 0.008. E: The pair distance distribution function, $P(r)$, for hIL-11 calculated from the raw data displayed in Figure 2B. The calculated volume of the scattering particle is $29,115 \text{ \AA}^3$. This volume corresponds to an approximate protein molecular weight of 18,200 Da, which is in good agreement with the expected molecular weight of 19,047 Da.

```

IL11_HUMAN      1  MNCVCRLVLVLVLSLWPLTAVAPGPEPGPRVSPDPRALDSTVLLTRSLLADTRQLAAQL
IL11_MOUSE      1  MNCVCRLVLVLVLSLWPLRVVAPGPEAGSPRVSSDPRALDSAVLLTRSLLADTRQLAAQM

IL11_HUMAN     61  RDKFPADGDHNLDDSLPTLAMSAGALGALQLPGVLRLRADLSYLRHVQWLRRAGGSSLK
IL11_MOUSE     61  RDKFPADGDHSLDDSLPTLAMSAGTLGSLQLPGVLRLRVDLSYLRHVQWLRRAGGPSLK

IL11_HUMAN    121  TLEPELGTLQARLRLLRRLQLLMSRLALPQPPDPPPAPPLAPPSSAWGGIRAAHAILGG
IL11_MOUSE    121  TLEPELGALQARLRLLRRLQLLMSRLALPQAAPDPVIPLGPPASAWGSIRAAHAILGG

IL11_HUMAN    181  LHLTLDWAVRGLLLLKTRL
IL11_MOUSE    181  LHLTLDWAVRGLLLLKTRL

```

Figure S3 Related to Figure 3. Sequence alignment of human IL-11 with mouse IL-11. The signal sequences of the two proteins (residues 1-21) are shown in italic font. The alignment was produced using the software CLUSTAL O.

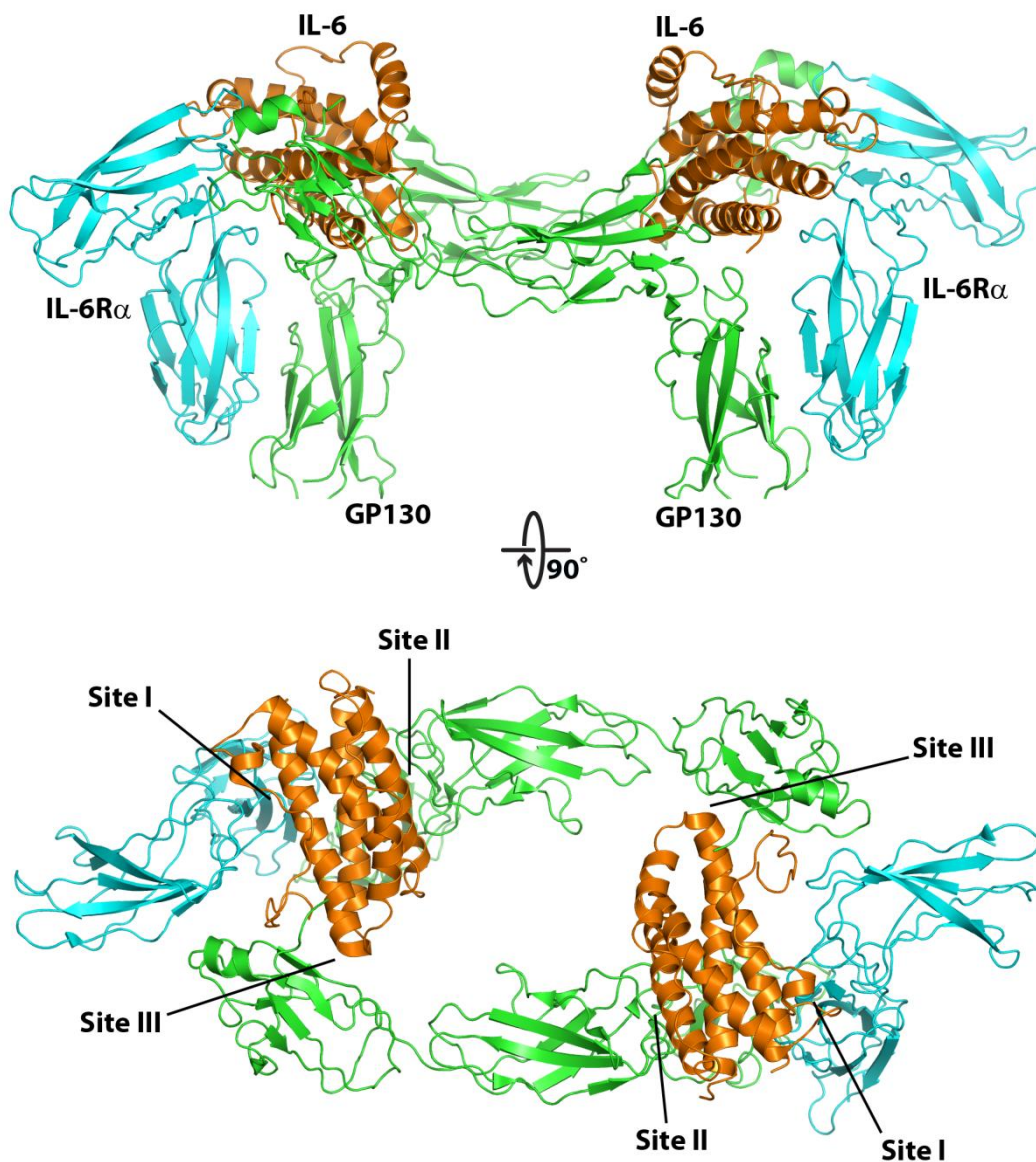


Figure S4 Related to Figure 3. Schematic representation of the structure of the hexameric IL-6/IL-6R α /GP130 complex (PDB ID: 1P9M). The complex contains two molecules each of IL-6 (orange) IL-6R α (cyan) and GP130 (green). IL-6 binds to IL-6R α via site I and to one molecule of GP130 via site II. The binding sites for IL-6 on each receptor are at the hinge region between the two fibronectin type III domains of the cytokine binding module. Each IL-6 molecule also binds to the second copy of GP130 via Site III, situated at one end of the 4-helix bundle.

```

IL11_HUMAN  1  MNCVC-----RLVLVLSLMEDTAVAPGPPPGPPRVSPDP-RAELDSTVLLT---RSL
IL6_HUMAN   1  MNSFSTSAFGPVAFSLGLLVLEAAFAFVPPGEDSRDVAAPHRQPLTSSERLDKQIRYI

IL11_HUMAN  50  LADTRQLAAQLRDK-----FPADGDHNLDSLPTLAMSAGALGA-LLPGVLTRLRADLL
IL6_HUMAN   61  LDGISALIRKETCNKSNMCESSKEALAENNLNLPKLAEKDGCFQSGFNEETCLVKITGLL

IL11_HUMAN  103 SYLRHVQWLRRAGGSSLKTLEPELGTLQARLDRLLRRLQ---LLMSRLALPQPPDPPAP
IL6_HUMAN   121 EHEVYLEVLQNRFESS---EQARAVQMSTKVLQFLOKKAKNLDALTTPDEPTNASLL

IL11_HUMAN  160 PLAPPSSAWGGIRAAHALLGGLLTLDWAVRCLLLKTRL
IL6_HUMAN   177 TKLQAQNQWLQDMTTHLLLRSFREELQSSLRALRQM-----

```

Figure S5 Related to Figure 4. Sequence alignment of human IL-11 with human IL-6. The signal sequences of the two proteins are shown in italic font. The alignment was produced using the software CLUSTAL O.

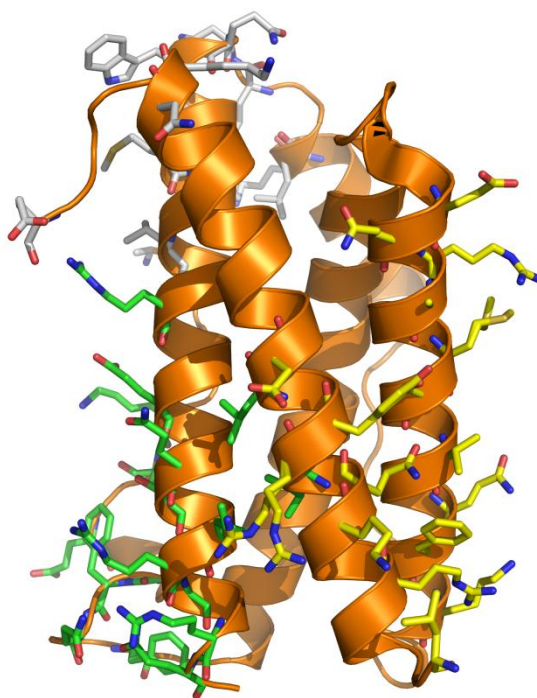


Figure S6 Related to Figure 4. The receptor binding regions of IL-6 (PDB ID: 1ALU). The program PISA was used to identify the residues of IL-6 in contact with IL-6R α and GP130 in the hexameric IL-6/IL-6R α /GP130 complex structure of IL-6 (PDB ID: 1P9M; Figure S3). Residues that form interface contacts with IL-6R α (green, site I) and the two molecules of GP130 (yellow, site II; grey, site III) are shown in stick representation (see also Figure S4).